AGU PUBLICATIONS

JGR

Journal of Geophysical Research: Biogeosciences

RESEARCH ARTICLE
10.1002/2014JG002794

Key Points:
- A Bayesian approach to isotopic partitioning of soil respiration is described
- Multiple sources of information are combined to quantify uncertainties
- Data-informed estimates of apparent fractionation effects are provided

Supporting Information:
- Supporting Information S1

Correspondence to:
K. Ogle,
Kiona.Ogle@asu.edu

Citation:
Ogle, K., and E. Pendall (2015), Isotope partitioning of soil respiration: A Bayesian solution to accommodate multiple sources of variability, *J. Geophys. Res. Biogeosci.*, *120*, 221–236, doi:10.1002/2014JG002794.

Received 4 SEP 2014
Accepted 27 DEC 2014
Accepted article online 6 JAN 2015
Published online 24 FEB 2015

Isotope partitioning of soil respiration: A Bayesian solution to accommodate multiple sources of variability

Kiona Ogle[1] and Elise Pendall[2,3]

[1]School of Life Sciences, Arizona State University, Tempe, Arizona, USA, [2]Hawkesbury Institute for the Environment, University of Western Sydney, Penrith, New South Wales, Australia, [3]Department of Botany and Program in Ecology, University of Wyoming, Laramie, Wyoming, USA

Abstract Isotopic methods offer great potential for partitioning trace gas fluxes such as soil respiration into their different source contributions. Traditional partitioning methods face challenges due to variability introduced by different measurement methods, fractionation effects, and end-member uncertainty. To address these challenges, we describe a hierarchical Bayesian (HB) approach for isotopic partitioning of soil respiration that directly accommodates such variability. We apply our HB method to data from an experiment conducted in a shortgrass steppe ecosystem, where decomposition was previously shown to be stimulated by elevated CO_2. Our approach simultaneously fits Keeling plot (KP) models to observations of soil or soil-respired $\delta^{13}C$ and $[CO_2]$ obtained via chambers and gas wells, corrects the KP intercepts for apparent fractionation (Δ) due to isotope-specific diffusion rates and/or method artifacts, estimates method- and treatment-specific values for Δ, propagates end-member uncertainty, and calculates proportional contributions from two distinct respiration sources ("old" and "new" carbon). The chamber KP intercepts were estimated with greater confidence than the well intercepts and compared to the theoretical value of 4.4‰, our results suggest that Δ varies between 2 and 5.2‰ depending on method (chambers versus wells) and CO_2 treatment. Because elevated CO_2 plots were fumigated with ^{13}C-depleted CO_2, the source contributions were tightly constrained, and new C accounted for 64% (range = 55–73%) of soil respiration. The contributions were less constrained for the ambient CO_2 treatments, but new C accounted for significantly less (47%, range = 15–82%) of soil respiration. Our new HB partitioning approach contrasts our original analysis (higher contribution of old C under elevated CO_2) because it uses additional data sources, accounts for end-member bias, and estimates apparent fractionation effects.

1. Introduction

Soil respiration is the largest source of CO_2 from terrestrial ecosystems to the atmosphere, amounting to nearly 100 Pg C in 2008, and it has been increasing in the past 20 years along with global temperatures [*Bond-Lamberty and Thomson*, 2010]. Application of isotopes to partition trace gas fluxes such as soil respiration (or soil CO_2 efflux) has provided important insights into the components governing such fluxes. Soil respiration is a composite of autotrophic respiration by roots and closely associated rhizosphere biota, and heterotrophic decomposition by soil microbes [*Hanson et al.*, 2000]. These processes have different biological and environmental drivers [*Bond-Lamberty et al.*, 2004; *Hanson et al.*, 2000] and are represented separately in most ecosystem and C cycle models [*Cox et al.*, 2000]. Although the partitioning of soil respiration into its two dominant sources is fraught with methodological difficulties [*Baggs*, 2006], isotopic methods are least invasive and could be considered least biased, because they have limited disruptive effects on the biological or environmental conditions surrounding the measurements [*Kuzyakov*, 2006].

Application of isotopes to partition soil respiration faces several challenges, and we highlight three important sources of variability: measurement approach, fractionation effects, and end-member uncertainty. The first two challenges are closely linked and affect our ability to obtain reliable estimates of the $\delta^{13}C$ of soil respiration ($\delta^{13}C_{SR}$). Gas samples collected from chambers that accumulate CO_2 respired from the soil surface [*Midwood and Millard*, 2011; *Risk et al.*, 2012] are assumed to reflect $\delta^{13}C_{SR}$ values in the absence of diffusive fractionation [*Amundson et al.*, 1998]. Soil CO_2 samples collected from gas wells buried at various depths in the soil [*Camarda et al.*, 2007; *Pendall et al.*, 2003, 2001], however, are subjected to diffusive fractionation.

Theory indicates that the $\delta^{13}C$ of the soil CO_2 should be enriched by up to 4.4‰ relative to $\delta^{13}C_{SR}$ due to fractionation associated with the difference in the diffusivity of $^{13}CO_2$ versus $^{12}CO_2$ [*Amundson et al*., 1998; *Cerling*, 1984]. However, the biophysical processes involved in soil CO_2 transport and efflux are rarely dominated by purely diffusive conditions at true steady state [*Kayler et al*., 2010a; *Moyes et al*., 2010]. Spatial or temporal changes in air-filled pore space, biological production, and atmospheric conditions such as $[CO_2]$ or wind speed can potentially induce apparent fractionation effects [*Kayler et al*., 2010a; *Moyes et al*., 2010; *Nickerson and Risk*, 2009c]. Buried gas wells, however, may be less subject to advective effects and other chamber artifacts [*Kayler et al*., 2010a; *Moyes et al*., 2010] and may provide more accurate estimates of $\delta^{13}C_{SR}$ if diffusive fractionation is accurately accounted for [*Amundson et al*., 1998].

With either approach, gas samples contain a mixture of CO_2 reflecting the background (atmospheric) air and CO_2 produced by biological processes within the soil. An approach developed in the 1950s [*Keeling*, 1958a] has been applied to estimate the $\delta^{13}C$ of the respired C source from ecosystems, soils, and plants [*Bowling et al*., 2008; *Pataki et al*., 2003]. Theoretically, the "Keeling plot" (KP) [*Keeling*, 1958b] intercepts from gas wells, but not chambers, and must be adjusted to account for diffusive fractionation [*Amundson et al*., 1998]. However, the theoretical value of 4.4‰ has rarely been measured in nature [*Kayler et al*., 2010a; *Quade et al*., 1989], and in fact, full diffusive fractionation may not occur due to commonly occurring advective conditions near the soil surface [*Bowling et al*., 2009]. Characterizing variation in the "apparent" fractionation factor—that is, the difference between $\delta^{13}C$ estimated from chamber or well samples versus the true source value of $\delta^{13}C_{SR}$—represents an ongoing research challenge [*Bowling and Massman*, 2011; *Bowling et al*., 2009; *Kayler et al*., 2010a].

The third challenge is to partition $\delta^{13}C_{SR}$ into its primary sources, which requires identifying appropriate values for the source end-members. Here we consider two end-members: $\delta^{13}C_{new}$, "new" or recently assimilated carbon (C), and $\delta^{13}C_{old}$, "old" C representing heterotrophic decomposition of soil organic matter. The distinction of these two sources is somewhat arbitrary because soil-respired CO_2 can be derived from a continuum of autotrophic (new C) to heterotrophic (old C) processes [*Högberg and Read*, 2006]. Nevertheless, quantifying the contribution of new C (derived from recently fixed photosynthate) versus old C (derived from microbial decomposition of old, dead substrate) is one of the primary challenges in C cycle research [*Heimann and Reichstein*, 2008]. The end-member isotopic values, however, are not necessarily constant or easily constrained. Thus, it is important to employ partitioning approaches that explicitly recognize such end-member uncertainty.

An analytical framework for isotopic partitioning of soil respiration that incorporates all relevant sources of uncertainty is needed. A spreadsheet approach (e.g., IsoError [*Phillips and Gregg*, 2001]) can be used to propagate errors associated with isotopic partitioning that accounts for variations in the mixture as well as the end-member $\delta^{13}C$ values. While this method has been successfully applied to soil respiration partitioning [*Pendall et al*., 2003], it lacks a statistical structure that allows identification of the various sources of uncertainty, including those highlighted above. Toward addressing these issues, Bayesian approaches have been developed that provide a coherent statistical framework for isotopic partitioning [*Moore and Semmens*, 2008; *Parnell et al*., 2010], but they have been primarily limited to studies of trophic interactions and diet partitioning [*Ogle et al*., 2013b]. These Bayesian approaches, however, are not structured to accommodate the simultaneous estimation of $\delta^{13}C_{SR}$ (e.g., via KP models), apparent fractionation effects, end-member uncertainty, and partitioning of soil respiration into its primary sources.

Thus, the goal of this study is to provide a rigorous modeling framework that is able to address the aforementioned challenges by integrating multiple sources of information, including data derived from multiple measurement methods (i.e., surface chambers and gas wells). In particular, we develop a hierarchical Bayesian (HB) model for simultaneously (1) analyzing the chamber and well $\delta^{13}C$ and $[CO_2]$ data in the context of KP models, (2) estimating the apparent fraction effect (Δ) without imposing theoretical values that may not be representative of the system, (3) propagating uncertainty in the end-members, and (4) estimating the proportional contributions from two distinct respiration sources (i.e., old and new carbon [C]). The HB approach directly accommodates the experimental design, allowing explicit assessment of different sources of uncertainty [*Clark*, 2003, 2005; *Ogle*, 2009]. Moreover, the coupling of the four aforementioned modules is accomplished via model modularization techniques [*Liu et al*., 2009; *Ogle et al*., 2013a] that control the feedback of information between the modules while simultaneously propagating uncertainty among modules. We describe our HB approach and apply it to an open-top chamber experiment conducted in a

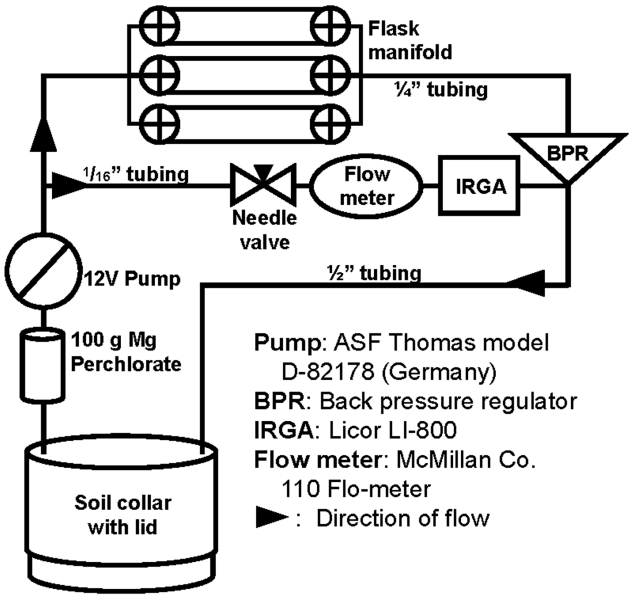

Figure 1. Nonsteady state chamber system for measuring soil respired [CO_2] and its isotopic composition. The PVC chamber was 20 cm in diameter and 10 cm tall. Three or four glass flasks (500 mL volume) were attached in parallel to the manifold. The chamber system was operated by first opening all stopcocks and filling all flasks and tubing with background air. The chamber was then sealed to the permanently installed base, and stopcocks on the first flask were closed. Soil respiration rates were calculated during the first 2 min from the increase in the [CO_2] measured on an infrared gas analyzer (IRGA) at 1 s intervals; however, these rates were not used in the present study. Additional flasks were collected after 3 and 6 min following closure (10 min for the fourth flask). An infrared gas analyzer (IRGA) recorded the increase in [CO_2] for the first 2 min at 1 s intervals. A magnesium (Mg) perchlorate trap was used to dry the air. Because the flasks were connected in parallel, flow was not altered, but the system volume was reduced when the flasks were closed.

shortgrass steppe ecosystem, where the original data analysis indicated that elevated CO_2 stimulated organic matter decomposition [*Pendall et al.*, 2003]. The current analysis adds previously unpublished chamber data to the original gas well data, allowing explicit estimation of Δ and providing new insights into effects of elevated CO_2 on soil respiration components.

2. Methods

Although our HB modeling approach can be applied in a variety of settings and modified to accommodate different sampling designs and data attributes, we describe our approach in the context of soil respiration data obtained from an elevated CO_2 experiment. Thus, we provide an overview of the field study, followed by a description of our modeling approach.

2.1. Field Measurements of Soil Respiration and δ^{13}C-CO_2

Our field data were obtained from an open-top chamber elevated CO_2 experiment conducted from 1997 to 2001 at the Shortgrass Steppe Long-Term Ecological Research site in northern Colorado. The ecosystem was dominated by a C4 grass (*Bouteloua gracilis*) and two C3 grasses (*Hesperostipa comata* and *Pascopyrum smithii*), with sandy loam soils [*Morgan et al.*, 2001]. Four treatments were imposed in native vegetation: ambient CO_2 chamber (AC), nonchamber ambient control (NC), elevated (doubled) CO_2 chamber (EC), and nonchamber fallow (F). The AC, NC, and EC chambers had three replicates each; the unreplicated F plot was established outside the chambers, and it lacked vegetation (via trenching and glyphosate application in 1998). The tank gas used to double the atmospheric [CO_2] had an approximate δ^{13}C value of -40‰, which produced air in the EC chambers of -24.7 ± 1.4‰, while background air had nearly constant δ^{13}C of -8.1 ± 0.2‰ [*Pendall et al.*, 2003].

Soil CO_2 isotope data were collected by two different methods (chambers and gas wells) to estimate the δ^{13}C of soil respiration ($\delta^{13}C_{SR}$), where each method is likely to be associated with differing degrees of apparent fractionation. *Pendall et al.* [2003] reported results based on a spreadsheet-type analysis of the gas well data, but this study is the first to use the chamber data. A chamber system was designed for collection of 0.5 L flasks without altering internal pressure or causing isotopic fractionation of respired CO_2 (Figure 1), and deployed on PVC bases (20 cm diameter inserted 2 cm deep into soil [*Mosier et al.*, 2003]). Soil gas wells (1.8 mm ID stainless steel tubing) were installed at depths of 3, 5, 10, 15, and 25 cm, from which soil air was collected in gas-tight syringes (3 cm^3 for 3 cm depth and 6 cm^3 for deeper wells), following a >30 min diffusion equilibration period [*Pendall et al.*, 2003]. Sampling for both methods was conducted between 10:00 and 14:00 local time, from all 10 plots on 10 dates in 1999 (5 and 26 May; 3, 16, and 30 June; 15 and 29 July; 3 August; 1 September; and 13 October).

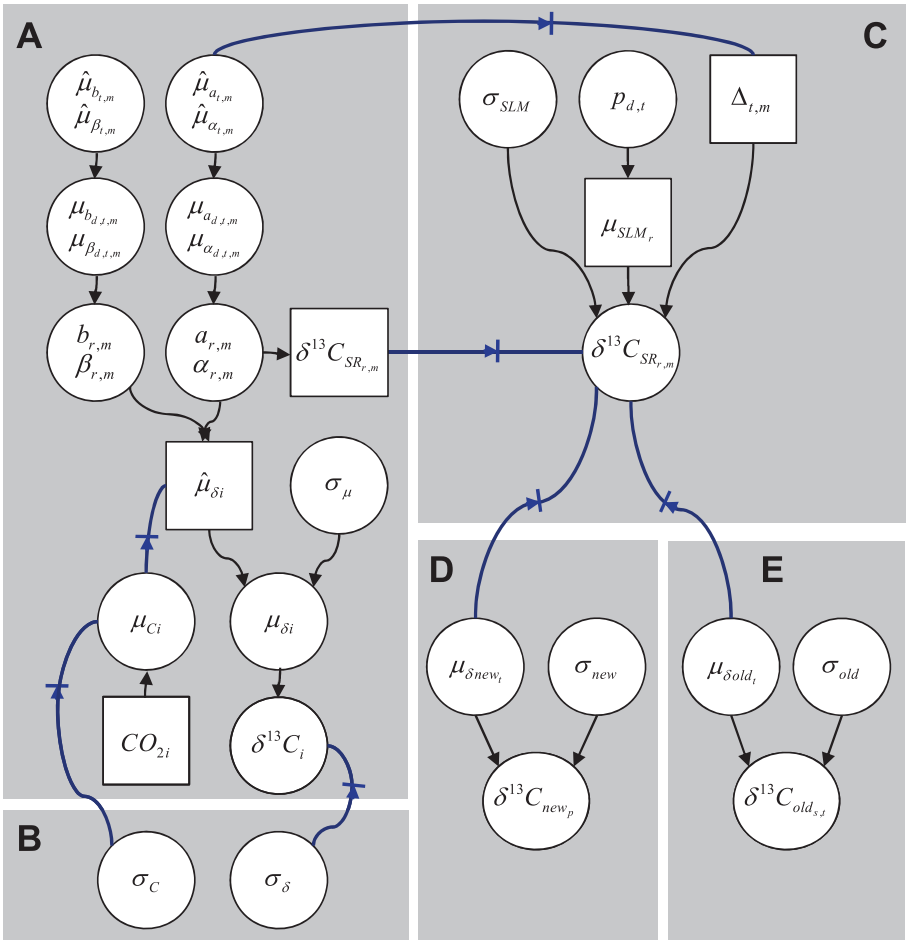

Figure 2. Graphical representation of the Bayesian model that combines submodels for the following: (a) Keeling plots that define the relationship between $\delta^{13}C$ and $[CO_2]$ of chamber and well air samples, (b) the calibration gas samples, (c) a simple linear mixing (SLM) model for partitioning soil respiration into its new and old C source contributions, (d) the new C end-member, and (e) the old C end-member. The subscripts and symbols in each submodel are defined in Table 1. The diode (valve) symbol (→|—) denotes feedback control such that (*a*) → |—(*b*) indicates that information or uncertainty about *a* is propagated to *b*, but *b* does not feedback to influence *a*. Circular nodes indicate stochastic quantities that are assigned distributions; square nodes indicate quantities that are fixed or deterministic functions of other quantities. See Figure S1 in the supporting information for a more detailed graphical model that corresponds to the detailed model described in Text S1 in the supporting information.

Samples from the gas wells were analyzed within 24 h for $[CO_2]$ on a LI 6200 infrared gas analyzer (Licor, Lincoln, NE) with precision of ±2 μmol mol^{-1} and for $\delta^{13}C$ on a Micromass Isoprime continuous flow isotope ratio mass spectrometer (Bristol, UK) fitted with a custom gas chromatograph inlet system, with precision of ±0.06‰. Flasks from the chamber system were analyzed for $[CO_2]$ by gas chromatography and for $\delta^{13}C$ by dual inlet isotope ratio mass spectrometry on a Micromass Optima. More details of the experimental setup can be found in *Pendall et al.* [2003]. Note that a balanced sampling design would have yielded 432 (nine dates × four treatments × four samples per KP × three replicates) chamber and 504 (seven dates × four treatments × six depths per KP × three replicates) gas samples, but due to logistical constraints and missing data, we obtained $[CO_2]$ and $\delta^{13}C$ data for 249 chamber and 293 well samples (total = 542).

2.2. Overview of Bayesian Modeling Approach

The primary goal of this study was to develop a modeling approach to simultaneously estimate the $\delta^{13}C$ of soil respiration ($\delta^{13}C_{SR}$) and to partition $\delta^{13}C_{SR}$ into its different source contributions. Our approach combines the following: (1) a hierarchical Keeling plot (KP) model, (2) an apparent fractionation model, (3) a respiration

Table 1. Description of Symbols Used in Manuscript, Their Associated Units (Data, Unknowns) or Range of Values (Indices), and the Equations That They Occur in

Symbol	Description	Units or Range of Values	Equations
	Indices		
d	Date	1, 2, …, 10	(6) and (7)
i	Observation	1, 2, …, 542	(1a)–(3)
m	Method	1 (chambers), 2 (wells)	(3)–(6)
q	Plot	1, 2, …, 9	(9)
r	Replicate	1, 2, …, 92	(3), (5), and (6)
s	Soil replicate	1, 2, 3, 4	(8)
t	Treatment	1 (AC), 2 (NC), 3 (EC), 4 (F)	(4)–(9)
	Data		
$\delta^{13}C$	^{13}C composition of gas sample	‰	(1a)
CO_2	CO_2 concentration of gas sample	$\mu mol\ mol^{-1}$	(1b)
	Unknowns		
a	Keeling plot (KP) intercept	‰	(3) and (5)
b	KP slope	‰ $\mu mol\ mol^{-1}$	(3)
p	Proportional contribution of new C	unitless, on interval [0, 1]	(7)
$\bar{p}$	Treatment-level average p	unitless, on interval [0, 1]	after (7)
Δ	Apparent fractionation	‰	(4) and (5)
$\delta^{13}C_{new}$	Empirical estimate of new ^{13}C end-member	‰	(9)
$\delta^{13}C_{old}$	Empirical estimate of old ^{13}C end-member	‰	(8)
$\delta^{13}C_{SR}$	^{13}C composition of soil respiration	‰	(5) and (6)
$\hat{\mu}_a$	Treatment/method-level KP intercept	‰	(4)
μ_C	Predicted $[CO_2]$ of gas sample	$\mu mol\ mol^{-1}$	(1b) and (3)
μ_δ	Predicted true $\delta^{13}C$ of gas sample	‰	(1a) and (2)
$\hat{\mu}_\delta$	KP predicted $\delta^{13}C$ of gas sample	‰	(2) and (3)
$\mu_{\delta new}$	Treatment-level new ^{13}C end-member	‰	(7) and (9)
$\mu_{\delta old}$	Treatment-level old ^{13}C end-member	‰	(7) and (8)
μ_{SLM}	Predicted $\delta^{13}C_{SR}$ from SLM model	‰	(6) and (7)
σ_C^2	CO_2 measurement error variance	$(\log[\mu mol\ mol^{-1}])^2$	(1b)
σ_δ^2	$\delta^{13}C$ measurement error variance	$(‰)^2$	(1a)
σ_{new}^2	Among plot variance of $\delta^{13}C^*_{new}$	$(‰)^2$	(9)
σ_{old}^2	Among plot variance of $\delta^{13}C^*_{old}$	$(‰)^2$	(8)
σ_μ^2	$\delta^{13}C$ process error variance	$(‰)^2$	(2)
σ_{SLM}^2	Among replicate variance of $\delta^{13}C_{SR}$	$(‰)^2$	(6)

isotope partitioning model, and (4) end-member models (Figure 2). The combined model is implemented in a hierarchical Bayesian (HB) framework that accommodates the experimental design involving measurements of soil or soil-respired CO_2 and $\delta^{13}C$ obtained via the two methods. The HB model assimilates data on soil CO_2 concentrations and associated $\delta^{13}C$ values; it does not explicitly utilize measurements of soil respiration. However, this model could be used in conjunction with soil respiration rate measurements to estimate new and old CO_2 fluxes in addition to their proportional contributions. Importantly, the HB approach allows for appropriate propagation of variability due to observation or measurement errors, parameter uncertainty, and natural variability inherent in the aforementioned four process components. In the following sections we highlight key aspects of our model, and Table 1 provides definitions of model quantities and subscript notation. A more detailed description of the model is given in Text S1 and Figure S2 in the supporting information.

2.3. Keeling Plot Model

Similar to existing approaches for fitting KP models [*Flanagan et al.*, 1996; *Pataki et al.*, 2003; *Zobitz et al.*, 2006], we assume that $\delta^{13}C$ and $[CO_2]$ are both measured with error. However, our approach differs from the least squares approach because we (1) treat both quantities ($\delta^{13}C$ and $[CO_2]$) as stochastic and assign likelihoods to each and (2) explicitly separate analytical measurement error and process error [e.g., *Ogle and Barber*, 2008; *Ogle et al.*, 2009]. We do not directly model $[CO_2]$, but we wish to account for uncertainty in the measured $[CO_2]$. Thus, we assume the typical notation for the likelihood of the observed $\delta^{13}C$, whereby the data ($\delta^{13}C_i$) vary about their latent (true) values ($\mu_{\delta i}$) (equation (1a)). We employ a Berkson-type model

[*Dellaportas and Stephens*, 1995] for the $[CO_2]$ data whereby the latent values (μ_{Ci}) vary about the data (CO_{2i}) (equation (1b)), thus allowing us to account for potential errors in the $[CO_2]$ measurements. For observation i ($i = 1, 2, \ldots, 542$), we assume that $\delta^{13}C$ and $[CO_2]$ follow a normal and lognormal distribution, respectively:

$$\delta^{13}C_i \sim \text{Normal}\left(\mu_{\delta_i}, \sigma_\delta^2\right) \tag{1a}$$

$$\ln\left(\mu_{C_i}\right) \sim \text{Normal}\left(\ln(CO_2)_i, \sigma_C^2\right) \tag{1b}$$

The variances ($\sigma_\delta{}^2$ and $\sigma_C{}^2$) quantify error associated with measuring the $\delta^{13}C$ and $[CO_2]$ of a gas sample.

Equations (1a) and (1b) can lead to nonidentifiability of the two variance terms. Thus, we used repeated measurements of a calibration gas with known $[CO_2]$ and $\delta^{13}C$ to separate $\sigma_\delta{}^2$ and $\sigma_C{}^2$ (see Text S1). Under the standard HB framework, data on both $\delta^{13}C$ and $[CO_2]$ would inform all unknown quantities in equations (1a) and (1b), but we only wish to propagate the analytical error associated with measuring $[CO_2]$. Thus, we "modularize" [*Liu et al*., 2009; *Ogle et al*., 2013a] the $[CO_2]$ model (equation (1b)) such that the $\delta^{13}C$ data do not feedback to influence the estimates of μ_C or $\sigma_C{}^2$ (Figure 2), which are thus only informed by the $[CO_2]$ data.

We assume that the observation-level mean $\delta^{13}C$ (μ_δ, equation (1a)) is normally distributed with an expected (mean) latent value of $\hat{\mu}_\delta$:

$$\mu_{\delta_i} \sim \text{Normal}\left(\hat{\mu}_{\delta_i}, \sigma_\mu^2\right) \tag{2}$$

where $\sigma_\mu{}^2$ describes process variability, which reflects sampling errors that can cause the true $\delta^{13}C$ and $[CO_2]$ to deviate from their expected relationship (see equation (3)). We model $\hat{\mu}_\delta$ as a function of the true $[CO_2]$ (μ_C, equation (1b)) via a linearized KP model by assuming that $\hat{\mu}_\delta$ is a mixture of the "source" (soil respiration) and the background (atmosphere) $\delta^{13}C$ [e.g., *Keeling*, 1958b; *Pataki et al*., 2003; *Zobitz et al*., 2006]:

$$\hat{\mu}_{\delta_i} = a_{r(i),m(i)} + b_{r(i),m(i)}\left(\frac{1}{\mu_{C_i}}\right) \tag{3}$$

where $r(i)$ and $m(i)$ indicate replicate r ($r = 1, 2, \ldots, 92$) and method m ($m = 1$ for chambers; $m = 2$ for wells) associated with observation i, respectively. The KP intercepts (a) are subsequently corrected for apparent fraction (see equation (5)) to obtain estimates of $\delta^{13}C_{SR}$.

For each method, the replicate-level KP samples were nested in date and treatment. Thus, we assigned hierarchical priors to the replicate-by-method level parameters (a and b) in equation (3) such that each is assumed to come from a normal distribution whose means (μ_a and μ_b; Figure 2) vary at the level of date, treatment, and method. We assigned hierarchical priors to μ_a and μ_b such that their means ($\hat{\mu}_a$ and $\hat{\mu}_b$; Figure 2) vary at the level of treatment and method (see Text S1 for additional details).

2.4. Apparent Fractionation Models

We are ultimately interested in estimating $\delta^{13}C_{SR}$, which requires that we correct the KP intercepts (a) for apparent fractionation (Δ, ‰). We explored different ways of estimating Δ, including assuming the same versus different Δ value for wells and chambers and/or allowing Δ to vary by treatment. The final model we focus on assumes that both methods capture the same "true" $\delta^{13}C_{SR}$, and differences in their KP intercepts should reflect different values of Δ. The chamber method (method $m = 1$) is expected to lead to little to no fractionation, and thus, we estimate a single stochastic Δ to allow for potential chamber artifacts that are likely to be independent of treatment. Given the relatively greater variability in the well CO_2 and $\delta^{13}C$ data and the potential for treatment-specific diffusive fraction effects, we allow Δ to vary by treatment t (i.e., for $m = 2$). Thus, we anchor the estimates of the Δ values around the chamber estimate such that for treatment t and method m, we assume the following:

$$\Delta_{t,m=2} = \Delta_{m=1} - \left(\hat{\mu}_{a_{t,m=1}} - \hat{\mu}_{a_{t,m=2}}\right) \tag{4}$$

where $\hat{\mu}_{a_{t,m}}$ represents the treatment-level KP intercept for each method (Figure 2). The chamber-specific Δ term ($\Delta_{m=1}$) is assigned a Uniform(0,15) prior; we choose the upper bound of 15 because it far exceeds the theoretical maximum of 4.4‰. The well Δ terms (i.e., $\Delta_{1,m=2}, \ldots, \Delta_{4,m=2}$) are computed via equation (4) given the estimates of $\Delta_{m=1}$ and each $\hat{\mu}_{a_{t,m}}$.

Finally, the replicate-level $\delta^{13}C_{SR}$ associated with each method is estimated as follows:

$$\delta^{13}C_{SR_{r,m}} = a_{r,m} - \Delta_{t(r),m} \quad (5)$$

where $t(r)$ denotes treatment t associated with replicate r, a is the KP intercept in equation (3), and $\Delta_{t,m}$ is given by equation (4) for $m = 2$ or by $\Delta_{m=1}$ for $m = 1$.

2.5. Isotope Partitioning Model

We simultaneously implement a simple linear mixing (SLM) model with isotope data to partition soil respiration with the above described KP model, thereby allowing us to propagate uncertainty in the $\delta^{13}C_{SR}$ estimates. The estimated $\delta^{13}C_{SR}$ values (equation (5)) are essentially treated like data in the SLM model, and we assume they are normally distributed:

$$\delta^{13}C_{SR_{r,m}} \sim \text{Normal}\left(\mu_{SLM_{d(r),t(r)}}, \sigma^2_{SLM}\right) \quad (6)$$

where $d(r)$ and $t(r)$ index the date d and treatment t associated with replicate r; σ^2_{SLM} describes the residual variation between replicates within each date-treatment combination given the predicted (or mean) $\delta^{13}C_{SR}$ value (μ_{SLM}, see equation (7)).

We followed *Pendall et al.* [2003] and focused on two potential sources contributing to soil respiration: microbial decomposition of old C and rhizosphere respiration of new C. We assume that the proportional contribution (p) of the new C source varies over time (sampling date) and between treatments but that it does not depend on method since $\delta^{13}C_{SR}$ has been corrected for the method-specific apparent fractionation (equation (5)). Without additional data to suggest otherwise, we use treatment-level new and old C end-members ($\mu_{\delta new}$ and $\mu_{\delta old}$, respectively) such that μ_{SLM} is defined as follows:

$$\mu_{SLM_{d,t}} = p_{d,t} \cdot \mu_{\delta new_t} + \left(1 - p_{d,t}\right) \cdot \mu_{\delta old_t} \quad (7)$$

We assigned Uniform(0,1) priors to each p and a wide uniform prior to σ_{SLM} in equation (6). We computed the treatment-level contribution of new C ($\overline{p}_t$) by averaging $p_{d,t}$ across all d for each t.

2.6. Propagating End-Member Variability

Long-term soil incubations with samples, collected from 5 to 15 cm and 30 to 45 cm depths, were used to quantify the old C end-member ($\delta^{13}C_{old}$). On 5 times during the "slow pool" decomposition phase (days 101, 122, 140, 171, and 199), respiration rates were measured for each incubation jar, and headspace CO_2 samples were collected from the jars and analyzed for [CO_2] and $\delta^{13}C$ [*Pendall and King*, 2007]. $\delta^{13}C_{old}$ was estimated for each replicate soil sample s ($s = 1, 2, 3, 4$) and treatment t by summing over the incubation flux-weighted estimates of the mean $\delta^{13}C$ obtained for each soil depth (two depths), while accounting for uncertainty in the fluxes and $\delta^{13}C$ values based on their standard errors. This yielded an empirical distribution of possible $\delta^{13}C_{old}$ values that vary at the level of s and t, and we assume that any particular value can be described as coming from a normal distribution with a mean, $\mu_{\delta old}$, that varies by treatment:

$$\delta^{13}C_{old_{s,t}} \sim \text{Normal}\left(\mu_{\delta old_t}, \sigma^2_{old}\right) \quad (8)$$

The treatment-level mean $\delta^{13}C_{old}$ ($\mu_{\delta old}$) is used in the SLM model in equation (7).

To estimate the new C end-member ($\delta^{13}C_{new}$), aboveground biomass and associated $\delta^{13}C$ values of leaves from the three most abundant species (*B. gracilis*, *P. smithii*, and *H. comata*) were measured at peak season. Because roots have higher $\delta^{13}C$ values than leaves, we used species-specific offsets to account for this effect on the new C source [*Pendall et al.*, 2004]. The isotopic composition of root respiration was not different from that of root tissue of these species sampled in a similar ecosystem (Figure S1 [*Carrillo and Pendall*, 2008]). We quantified $\delta^{13}C_{new}$ for each plot q ($q = 1, 2, \ldots, 9$) and treatment t by summing the biomass-weighted leaf $\delta^{13}C$ values of these three species, and subsequently adjusting for the difference between leaf and root $\delta^{13}C$ to obtain an estimate of $\delta^{13}C_{new}$. We propagated uncertainty in the biomass, leaf $\delta^{13}C$, and leaf versus root $\delta^{13}C$ offsets based on their empirical standard errors, yielding an empirical distribution of possible values

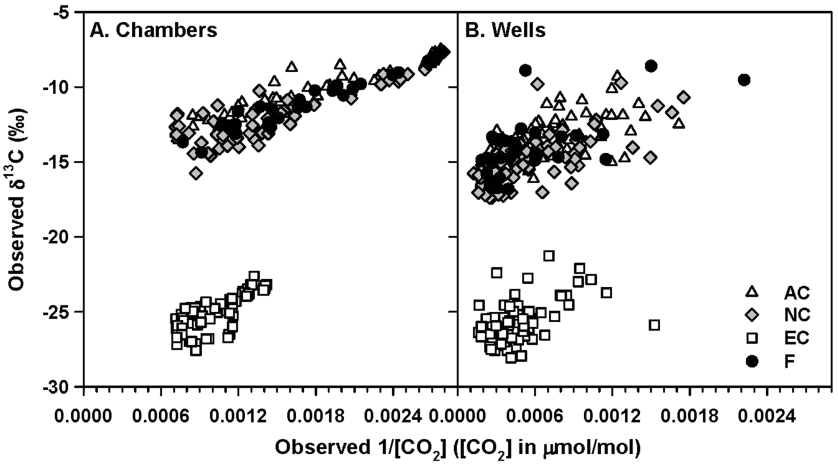

Figure 3. Observed $\delta^{13}C$ versus observed $1/[CO_2]$ for each observation *i*: (a) chambers and (b) gas wells. The treatments are indicated by AC (ambient CO_2 chamber), NC (ambient nonchamber control), EC (elevated CO_2 chamber), and F (nonchamber fallow control).

for$\delta^{13}C_{new}$ that vary at the level of *q*; we assume that any particular plot-level value can be described as coming from a normal distribution with a mean, $\mu_{\delta new}$, that varies by treatment:

$$\delta^{13}C_{new_q} \sim \text{Normal}\left(\mu_{\delta new_{t(q)}}, \sigma^2_{new}\right) \quad (9)$$

where $t(q)$ denotes treatment *t* associated with plot *q*; the treatment-level mean $\delta^{13}C_{new}$ ($\mu_{\delta new}$) is used in the SLM model in equation (7).

End-member data were not available for the fallow (F) treatment, thus we set $\mu_{\delta old}$ and $\mu_{\delta new}$ of the F treatment equal to that of the NC control. We modularized the end-member models so that the KP data do not feedback to affect the estimates of $\mu_{\delta old}$ and $\mu_{\delta new}$ (i.e., only the end-member data inform $\mu_{\delta old}$ and $\mu_{\delta new}$), but uncertainty in these end-members is propagated to the SLM model in equation (7) (for more details, see Text S1).

2.7. Model Implementation

The model was implemented in OpenBUGS [*Lunn et al.*, 2009a], and we modularized model components by using the built-in cut function [*Lunn et al.*, 2009a; *Ogle et al.*, 2013a]. The Markov chain Monte Carlo simulation details are given in Text S1 in the supporting information, and the OpenBUGS code is provided in Text S2. We evaluated model fit for the KP component by comparing observed versus predicted $\delta^{13}C$ [*Gelman et al.*, 2004].

3. Results

3.1. Model Fit

The observed $\delta^{13}C$ and CO_2 of the chamber samples were closer to background air and less variable compared to the well samples (Figure 3). The model fit was slightly better for the chamber data ($R^2 = 0.999$; Figure 4a) compared to the well data ($R^2 = 0.984$; Figure 4b). The wells, however, produced a sampling error standard deviation (σ_μ, equation (2)) that was 3 times higher than the chamber data (compare the widths of the 95% credible intervals (CIs) for the replicated data; Figure 4a versus Figure 4b).

3.2. The $\delta^{13}C$ of Soil-Respired CO_2

The replicate-level KP intercepts (*a*, equation (3)) spanned a greater range of values for chambers compared to the wells (see variation in posterior *means* for *a*, Figure 5), but the *uncertainty* in the *a* estimates was greater for the wells such that their 95% CIs were on average 50% (EC treatment) and 71–84% (AC, NC, and F) wider than the 95% CIs for the chambers. Moreover, the *a* estimates often differed between the chambers and wells, and these differences depended on CO_2 treatment (Figure 5). For example, *a* was generally higher (more enriched in ^{13}C) for the chambers compared to the wells in the AC treatment (Figure 5a), but wells

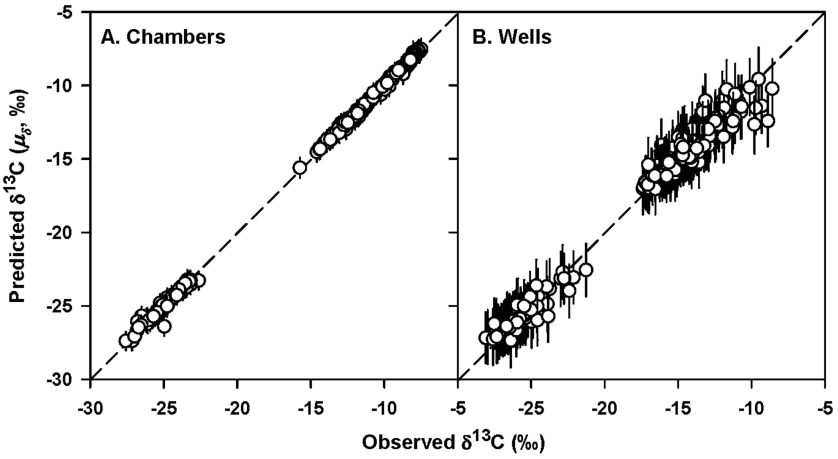

Figure 4. Evaluation of model fit with respect to the Keeling plot (KP) component (see Figure 2a) that involves the chamber and well $\delta^{13}C$ and [CO_2] data. Observed versus predicted $\delta^{13}C$ for each observation *i* for: (a) chambers and (b) gas wells. Predicted values are the posterior means and 95% credible intervals (CI) of replicated data obtained by generating observation-level values of $\delta^{13}C$ from equation (1a), which is linked to the KP model in equation (3). The diagonal dashed line is the 1:1 line.

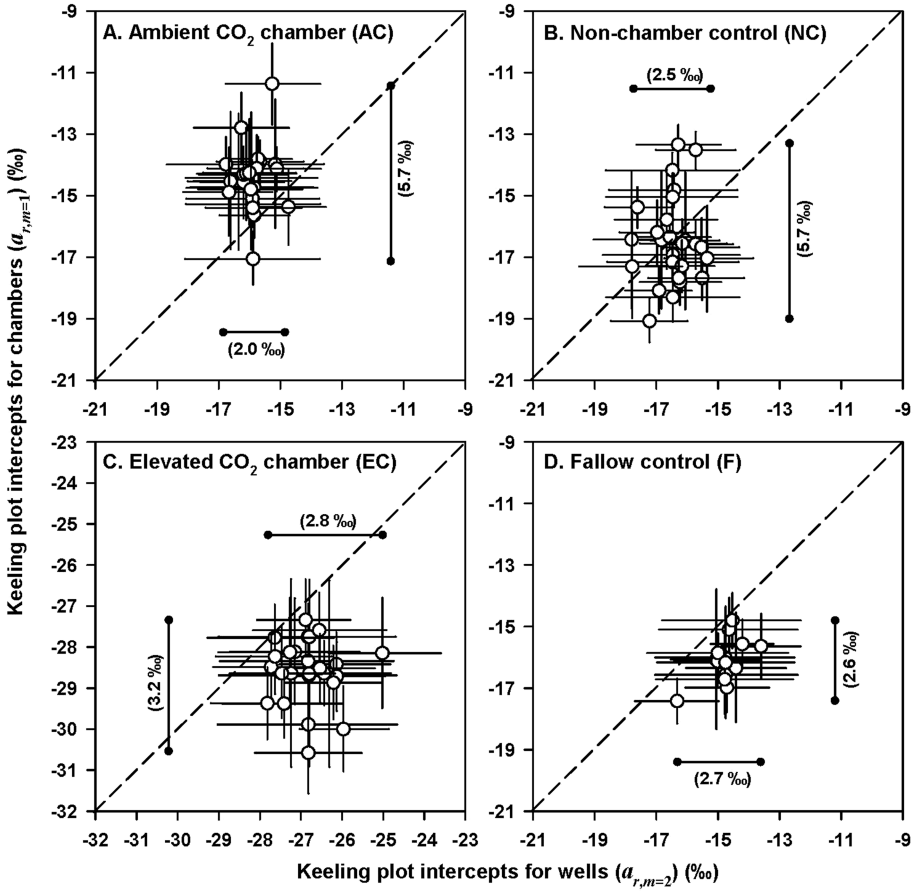

Figure 5. Posterior means and 95% credible intervals (CIs) for the replicate-level Keeling plot intercepts (i.e., $a_{r,m}$ in equation (3)) based on the chambers ($m = 1$) versus the wells ($m = 2$) for each CO_2 treatment: (a) ambient CO_2 chamber (AC), (b) nonchamber ambient control (NC), (c) elevated CO_2 chamber (EC), and (d) fallow ambient control (F). The diagonal dashed lines are the 1:1 lines. The vertical (chambers) and horizontal (wells) bars in each panel depict the range of values (‰) that the *posterior means* span, with the actual range (maximum mean — minimum mean) given in parentheses. Differences in the uncertainty associated with each intercept estimate ($a_{r,m}$) are determined by evaluating the *widths* of the *individual 95% CIs*; on average, the 95% CIs were 72% (AC), 71% (NC), 50% (EC), and 84% (F) wider for the wells compared to the chambers.

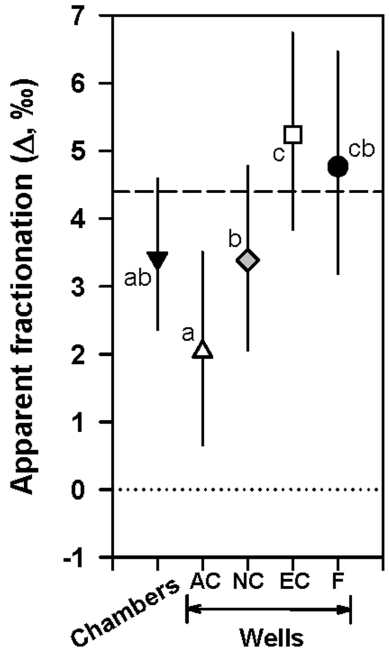

Figure 6. Posterior means and 95% credible intervals (CIs) for the apparent fraction effect (Δ in equation (4)), where a single Δ is estimated for the chambers, and treatment-level Δ terms are estimated for the wells. See Figure 5 for treatment definitions. Different letters (a, b, and c) indicate that the Δ term differed significantly (at the 5% level) between the corresponding methods and/or treatments. The horizontal dashed line indicates the theoretical value of Δ = 4.4‰; the horizontal dotted line represents Δ = 0‰.

weremore enriched in the EC and F treatments (Figures 5c and 5d). This treatment-dependent discrepancy between the methods suggests that apparent fractionation (Δ) may have varied by method and treatment. The model produced realistic estimates of Δ; all five Δ terms—one Δ for the chambers ($\Delta_{m=1}$) and four treatment-specific Δ's for the wells ($\Delta_{t,m=2}$)—were significantly greater than zero, and four Δ terms did not differ significantly from 4.4‰ (Figure 6). It appears, however, that Δ differs among treatments for the wells, with Δ being lowest (posterior mean = 2.0‰) for the AC treatment and highest for the EC treatment (posterior mean = 5.2‰). The chamber Δ estimate (posterior mean = 3.4‰) was intermediate between the well estimates and was significantly greater than the theoretically expected 0‰ (Figure 6).

3.3. Partitioning Soil Respiration

Across all treatments, the replicate-level posterior means of $\delta^{13}C_{SR}$ were generally contained within the range of the old and new C end-members (see Figure 7 for the chambers and Figure S3 for the wells). The application of CO_2 depleted in ^{13}C to the EC plots resulted in a wide separation (difference of ~19‰) of $\delta^{13}C_{old}$ and $\delta^{13}C_{new}$ (i.e., of the treatment-level means, $\mu_{\delta old}$ and $\mu_{\delta new}$, respectively; Figure 7c). Conversely, $\mu_{\delta old}$ and $\mu_{\delta new}$ were only separated by about 4.7‰ in the three ambient treatments (AC, NC, and F), and many of the 95% CIs for the replicate-level $\delta^{13}C_{SR}$ values overlapped the 95% CIs of both $\mu_{\delta old}$ and $\mu_{\delta new}$ in the three ambient treatments (Figures 7a, 7b, and 7d). Within the EC treatment, the 95% CIs for each replicate-level $\delta^{13}C_{SR}$ also fell well within the range of the $\mu_{\delta old}$ and $\mu_{\delta new}$ values (Figure 7c).

The date- by treatment-level estimates of the contribution of new C (p, equation (7)) did not exhibit any clear temporal patterns (see Figure S4 in the supporting information). Thus, we computed the treatment-level contributions of new C ($\overline{p}$) and old C ($1-\overline{p}$). In the EC treatment, the posterior estimates of $\overline{p}$ are well constrained, with a posterior mean of 0.64 and a relatively narrow 95% CI (0.55, 0.73) (Figure 8). Under ambient CO_2, the posterior mean for $\overline{p}$ ranged from 0.36 (AC treatment) to 0.57 (NC treatment), but the 95% CIs were >2.5 times wider compared to the EC treatment (Figure 8). Despite this large uncertainty, the contribution of new C was significantly lower under the AC compared to the EC treatment (the associated treatment-level posterior mean for $\overline{p}$ was not contained in the other treatment level's 95% CI for $\overline{p}$).

4. Discussion

4.1. Bayesian Solution to Isotopic Partitioning of Soil Respiration

We describe a flexible hierarchical Bayesian (HB) approach for isotopic partitioning of ecosystem fluxes, with specific application to soil respiration. The approach directly accommodates and partitions multiple sources of variability affecting the estimates of soil-respired $\delta^{13}C$ ($\delta^{13}C_{SR}$) and its different sources. Here we focus on partitioning the contribution of old and new C sources, but other sources can be accommodated given appropriate data. Our approach involves a Keeling plot (KP) submodel that is applied to replicate sets of $\delta^{13}C$ and [CO_2] data obtained by different methods (e.g., chambers and gas wells), and it simultaneously corrects

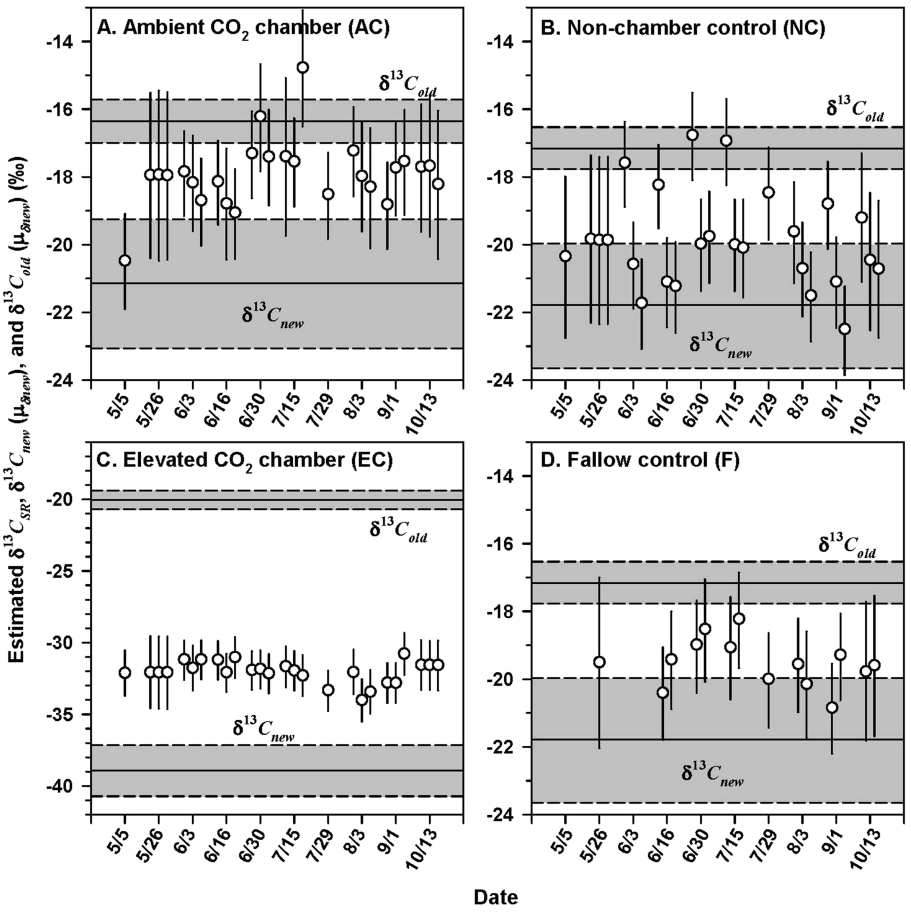

Figure 7. Posterior means and 95% credible intervals (CIs) for the estimated $\delta^{13}C$ of soil respiration ($\delta^{13}C_{SR}$, equstion (5)) for each sampling date overlaid with the treatment-level $\delta^{13}C$ of the old and new C end-members, $\mu_{\delta old}$ (equation (8)) and $\mu_{\delta new}$ (equation (9)), respectively. The range of values for each end-member is indicated by the horizontal gray region; the solid horizontal line indicates the posterior mean and the dashed lines the 95% CI. The $\delta^{13}C_{SR}$ results are based on the chamber data for each CO_2 treatment level.

the KP intercepts for apparent fractionation effects (Δ). The Δ terms are simultaneously estimated such that the estimated $\delta^{13}C_{SR}$ values fall within the range of the potential end-members (including variations in $\delta^{13}C_{old}$ and $\delta^{13}C_{new}$). The approach also propagates end-member uncertainty, which is informed by complimentary data or experiments. An important aspect of the HB approach is the ability to control feedback between the submodels by modularizing specific model components [*Ogle et al.*, 2013a]. For example, the stochastic end-member models are modularized so that the soil $[CO_2]$ and $\delta^{13}C$ data do not feedback to affect the $\delta^{13}C_{old}$ and $\delta^{13}C_{new}$ estimates. From the perspective of the SLM model that is used to partition soil respiration, $\delta^{13}C_{old}$ and $\delta^{13}C_{new}$ are viewed as distributional constants [*Lunn et al.*, 2009b; *Ogle et al.*, 2013a] that are not updated by the $[CO_2]$ and $\delta^{13}C$ data.

The HB approach to fitting the KP models to the $\delta^{13}C$ and $[CO_2]$ data improves upon previous approaches because it does not make any assumptions about the relative magnitude of the $\delta^{13}C$ and $1/[CO_2]$ analytical or measurement error variances. For example, *Pataki et al.* [2003] recommended using Model II regression that acknowledges measurement error in the covariate data (i.e., $1/[CO_2]$) and is thus expected to provide unbiased estimates of the KP intercepts. Conversely, *Zobitz et al.* [2006] suggest that Model II approaches yield biased estimates because their assumptions about the relative sizes of the $\delta^{13}C$ and $1/[CO_2]$ measurement error variances (e.g., Model II assumes nearly equal variances) are inappropriate; thus, they advocate using Model I regression (i.e., ordinary least squares). *Kayler et al.* [2010b] propose a potential solution by suggesting the use of Model II regression when the range of $[CO_2] > 1000\ \mu mol/mol$. Unlike

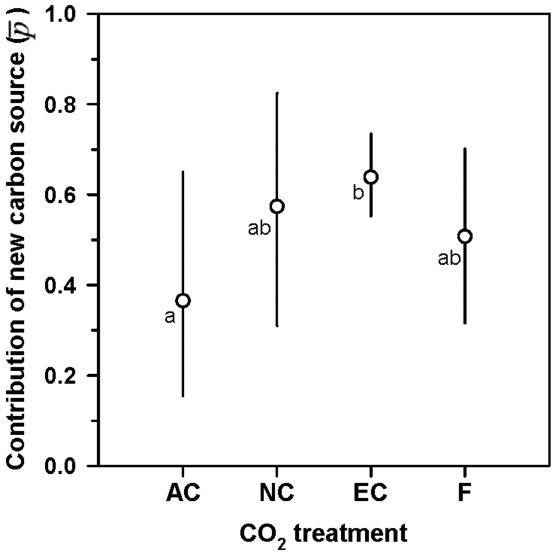

Figure 8. Posterior means and 95% credible intervals (CIs) for the treatment-level contribution of new C ($\bar{p}$) to soil respiration for each CO_2 treatment level; see Figure 5 for treatment definitions. The overall contributions were computed as the mean p (see equation (7)) across all dates within each treatment. Different letters (a and b) indicate that $\bar{p}$ differed significantly (at the 5% level) among the corresponding treatments.

Model I and Model II regressions, the flexibility of the Bayesian approach allowed us to model variation in log(CO_2), as captured by σ_C. Based on distribution theory and transformation of variables [*Casella and Berger*, 2002], we can derive posterior estimates of the variance in the linear predictor (σ^2_X), 1/[CO_2], which differed by 9–11 orders of magnitude compared the variance in the response, $\delta^{13}C$, $\sigma^2{}_\delta$ (posterior means: $\sigma^2{}_\delta = 8.27 \times 10^{-3}$ and $\sigma^2{}_X$ ranged from 1.16×10^{-14} when [CO_2] ≅ 8000 μmol/mol to 5.71×10^{-12} when [CO_2] ≅ 360 μmol/mol). Moreover, modularization of the calibration data model enabled us to obtain identifiable estimates of σ_δ, σ_C, σ_X, and other sources of error associated with measuring and modeling $\delta^{13}C$ (e.g., as quantified by σ_μ, equation (2)).

Our HB submodel for partitioning soil respiration shares similarities with recent Bayesian SLM models that have mostly been applied to partitioning animal diets [*Ogle et al*., 2013b]. These approaches include the MixSIR [*Moore and Semmens*, 2008] and Stable Isotope Analysis in R (SIAR) [*Parnell et al*., 2010] algorithms, which are constructed to assimilate data on the $\delta^{13}C$ of the mixture (e.g., $\delta^{13}C_{SR}$) and the end-members (e.g., $\delta^{13}C_{old}$ and $\delta^{13}C_{new}$). They also assign priors to the proportional contributions (p, equation (7)), and the Bayesian framework allows for incorporation of informative priors, which, in the diet partitioning studies, can be constructed based on other sources of information such as gut contents [*Moore and Semmens*, 2008; *Yeakel et al*., 2011]. Here we do not have independent sources of information to justify informative priors, but the HB model can easily accommodate a change in the prior specifications for p or any other model parameter. In contrast to the SIAR and MixSIR approaches, our HB approach couples stochastic models, via the modularization techniques, for estimating the $\delta^{13}C$ of the mixture (i.e., we do not have direct observations on $\delta^{13}C_{SR}$) and of the end-members.

4.2. Sources of Variation: Measurement Methods

Quantification of the sources of soil respiration is highly method dependent [*Hanson et al*., 2000]. Stable isotope partitioning studies generally apply either a chamber-based approach or gas wells, which have different advantages and disadvantages. Our data indicated less variability in observed $\delta^{13}C$ of CO_2 from chambers (Figure 3a) than gas well samples (Figure 3b), but the gas well observed $\delta^{13}C$ values were generally closer to the y intercept than the chamber observations due to their higher [CO_2] values (lower 1/[CO_2]). We suspect that the gas well data were more variable owing to the small spatial scale on which they were collected (a volume with ~2 cm radius assuming 50% porosity), in comparison to the larger spatial scale of chambers (10 cm radius area). Small-scale variations in root distribution, animal burrows, etc. were likely more apparent in gas well $\delta^{13}C$ values than in the more spatially representative chambers. Overall, these method-specific data characteristics caused the chamber KP intercepts to be estimated with greater confidence (narrower CIs) than the well intercepts, especially under ambient CO_2 conditions (Figure 5).

The comparatively large uncertainty (wide CIs) in the predicted gas well observations (Figure 4b) and corresponding KP intercepts (Figure 5) likely reflects natural spatial heterogeneity on the small scale of the sample volumes (3–6 mL). By contrast, the larger volume sampled in the chambers (500 mL) reflects continuously accumulating CO_2 flux from the same location (area = 0.3 m^2), resulting in narrower CIs for each

predicted chamber observation (Figure 4a) and corresponding KP intercepts (Figure 5). Across the entire study period, the chambers sampled greater natural temporal variability in the soil system than the wells (Figure 5). This wider range may also indicate a greater influence from advective effects [*Kayler et al*., 2010a], lateral diffusion, and/or air-to-chamber feedback [*Nickerson and Risk*, 2009a, 2009b]. Because the chamber closure periods were usually just 6 min, the effect of these artifacts was expected to be small. However, the high diffusivity of the sandy soil in our study may have facilitated these effects [*Nickerson and Risk*, 2009b] and led to the estimated apparent fractionation of 3.4‰ for chambers (Figure 6).

4.3. Sources of Variation: Apparent Fractionation

Applying stable C isotopes to partitioning soil respiration into its different C sources should account for both physical and biological effects on the $\delta^{13}C$ values within the system. The theoretical diffusion fractionation of 4.4‰ [*Amundson et al*., 1998; *Cerling et al*., 1991] has rarely been observed in nature, and estimates of Δ are generally lower than 4.4‰, probably owing partly to advective effects associated with wind pumping, which diminishes the purely diffusive fractionation effect [*Bowling and Massman*, 2011; *Bowling et al*., 2009]. Here we combined data generated from gas wells and chambers to simultaneously estimate both Δ and the true $\delta^{13}C$ of soil respiration ($\delta^{13}C_{SR}$). Our estimates of Δ (Figure 6) were physically realistic and in agreement with other estimates [e.g., *Kayler et al*., 2010a]. Our results indicate that Δ can vary by method and treatment and that this variation must be accounted for to obtain valid partitioning results. We note, however, that our HB approach could be extended to include greater process representation and potentially more refined estimates of Δ and the source contributions (*p*'s) [*Ogle et al*., 2013b], provided requisite data are available. In particular, one could explicitly incorporate a CO_2 advection-diffusion model [*Cerling et al*., 1991; *Fang and Moncrieff*, 1999] to help constrain Δ and separate the effects of purely diffusive, advective, and other fractionating factors. Such refinements, however, introduce implementation challenges given that existing Bayesian packages such as OpenBUGS cannot easily accommodate such complexity.

4.4. Sources of Variation: End-Member Uncertainty

Research over the last 5 years has provided substantial evidence for strong variability in $\delta^{13}C$ values of respiratory sources, which we use as end-members for soil respiration partitioning. For the purpose of this study, we employed three main simplifications regarding end-member variability: (1) source $\delta^{13}C$ values are constant over time, (2) source CO_2 $\delta^{13}C$ can be estimated from tissue biomass $\delta^{13}C$, and (3) there are a small and finite number (i.e., two) of end-members. Further development of our HB approach can allow for refinements to these assumptions by modifying the end-member models accordingly and propagating uncertainties in the end-member estimates via the aforementioned modularization techniques.

Our assumption of time-constant old and new end-members is a simplification of a dynamic process. The old C end-member $\delta^{13}C$ in our study was based on long-term incubations of root-free soil, under optimal moisture and temperature conditions, and was lower than that of the bulk organic matter [*Pendall and King*, 2007]. The $\delta^{13}C$ of heterotrophic respiration measured in root exclusion plots was observed to be constant in spruce forest [*Risk et al*., 2012] but to vary by at least 4‰ in a maple forest [*Moyes et al*., 2010]. Moreover, the $\delta^{13}C$ respired from our fallow (F) plots fell between the $\delta^{13}C$ values of the old and new C end-members, indicating that in the fallow plots, turnover of roots continued to contribute to soil respiration (~50% in our case; Figure 8).

The $\delta^{13}C$ of photosynthetic substrates is variable due to physiological responses to environmental variations, primarily soil moisture or relative humidity, light, and temperature [*Bowling et al*., 2008]. Physiological fractionation of ^{13}C in respired substrates appears to be less important in root- than leaf-respired $\delta^{13}C$ [*Bathellier et al*., 2009]. Dry conditions decouple photosynthesis and soil respiration [*Shim et al*., 2009], indicating that incorporating seasonal variations in $\delta^{13}C_{new}$ may be more important in mesic than xeric ecosystems. Our assumption that $\delta^{13}C_{new}$ could be estimated from C3 and C4 root tissue $\delta^{13}C$ is supported by data from a similar ecosystem [*Carrillo and Pendall*, 2008]. However, understanding of $\delta^{13}C$ of root and microbial respiration is still evolving [*Werth and Kuzyakov*, 2010].

A further simplification is related to the assumption that soil respiration can be divided into two main sources. In fact, substrates used in respiratory processes span a continuum of quality, turnover rate, and isotopic composition [*Bowling et al*., 2008; *Werth and Kuzyakov*, 2010]; and furthermore, the distinction between autotrophic and heterotrophic processes is somewhat arbitrary [*Högberg and Read*, 2006]. For instance, our

fallow (F) plot $\delta^{13}C$ value may represent substrate with an intermediate turnover rate between the old and new C end-members (Figure 7d); alternatively, it may represent a mixture of the new and old end-member values. Labeling experiments could provide the required information to distinguish multiple substrate sources and establish sufficient isotopic offsets for partitioning [*Gamnitzer et al*., 2011]. A more process-based approach to partitioning soil respiration could include detailed physiological measurements on source-specific respiratory fluxes, activity, biomass, or ^{13}C content and discrimination to help distinguish multiple sources and their potential spatial and temporal variability [*Ogle et al*., 2004, 2013b; *Zobitz et al*., 2007]. Importantly, the HB modularization approach described here can be easily modified to accommodate greater process detail, such as temporal variations in end-member values.

4.5. Ecological Implications of Isotope Partitioning Methods

In the original analysis of our gas well data [*Pendall et al*., 2003], the EC treatment was found to have a significantly greater proportion of respiration derived from decomposition (old C) than the AC treatment [*Pendall et al*., 2003]. By contrast, in the current analysis, a significantly greater proportion of respiration was derived from new C in the EC compared to the AC treatment (Figure 8), leading to the opposite ecological interpretation from the original results. This result suggests that the main effect of increasing atmospheric CO_2 in this ecosystem was to stimulate the rate of new C turnover [*Hungate et al*., 1997]. Our new analysis is consistent with increased active and slow pool C in topsoil, as estimated from laboratory incubation of soil from this experiment [*Pendall and King*, 2007]. Although total soil C content was not significantly affected by elevated CO_2 in this experiment, rhizodeposition was doubled [*Pendall et al*., 2004], also consistent with increased rates of new C cycling as determined in the present analysis. Ideally, net ecosystem productivity (NEP) should be constrained with stable isotopes to track both inputs of new C and losses of old C [*Pendall et al*., 2005]. Applying our new estimate of heterotrophic respiration to the original data on pools and fluxes, we found that EC plots accumulated about 10 g C m^{-2} yr^{-1}, while the AC plots lost about 90 g C m^{-2} yr^{-1} during the 1999 growing season, which is in contrast to estimated NEP in the original study of about 50 g m^{-2} yr^{-1} [*Pendall et al*., 2005].

Clearly, the application of stable isotope tracers to resolving small changes in NEP is powerful but dependent upon data analysis assumptions [e.g., *Kayler et al*., 2010a]. In this case, the contrasting outcomes can be explained by at least three differences in the analyses. First, the 2003 paper was based only on gas wells, whereas our current contribution is influenced by both chambers and gas wells. Second, the new end-member $\delta^{13}C$ was not originally corrected for the root-leaf offset as we did here. Third, Δ was considered to be 4.4‰ for all treatments in the 2003 paper whereas here we combine methods to estimate method- and treatment-specific Δ values.

In summary, our current approach provides several improvements over the original analysis, which is how most researchers treat their data. The HB method explicitly estimates Δ, considers multiple data streams, and accounts for and quantifies multiple sources of variation, thus likely producing more realistic error or uncertainty estimates. In summary, ecological interpretations of soil respiration partitioning should be considered cautiously, since they are still dependent on the field and statistical methods used. Despite its uncertainties, the isotope partitioning method is still less disruptive to belowground processes involved in soil CO_2 efflux than other common methods such as root exclusion [*Kuzyakov*, 2006]. Further investigation of climatic change impacts on soil C cycling should combine stable isotopic analysis with suitable statistical methods to reduce uncertainties in predictions of future carbon-climate feedbacks.

Acknowledgments
This material is based upon work supported by the USDA-CSREES Soil Processes Program (2008-35107-18655), U.S. Department of Energy Office of Science (BER), through the Terrestrial Ecosystem Science program (DE-SC0006973) and the Western Regional Center of the National Institute for Climatic Change Research, and by the National Science Foundation (DEB1021559). Any opinions, findings, and conclusions or recommendations expressed in this material are those of the author(s) and do not necessarily reflect the views of the National Science Foundation. We thank Levi Davis for assisting with implementing models in OpenBUGS and Colin Tucker and Ming Nie for providing comments on a previous version of this manuscript. A subset of data used in this study is provided in Text S2 in the supporting information, and complete data sets are freely available through DRYAD (http://datadryad.org/).

References

Amundson, R., L. Stern, T. Baisden, and Y. Wang (1998), The isotopic composition of soil and soil-respired CO_2, *Geoderma*, *82*(1–3), 83–114.
Baggs, E. M. (2006), Partitioning the components of soil respiration: A research challenge, *Plant Soil*, *284*(1–2), 1–5.
Bathellier, C., G. Tcherkez, R. Bligny, E. Gout, G. Cornic, and J. Ghashghaie (2009), Metabolic origin of the $\delta^{13}C$ of respired CO_2 in roots of *Phaseolus vulgaris*, *New Phytol.*, *181*(2), 387–399.
Bond-Lamberty, B., and A. Thomson (2010), Temperature-associated increases in the global soil respiration record, *Nature*, *464*(7288), 579–U132.
Bond-Lamberty, B., C. K. Wang, and S. T. Gower (2004), A global relationship between the heterotrophic and autotrophic components of soil respiration?, *Global Change Biol.*, *10*(10), 1756–1766.
Bowling, D. R., and W. J. Massman (2011), Persistent wind-induced enhancement of diffusive CO_2 transport in a mountain forest snowpack, *J. Geophys. Res.*, *116*, G04006, doi:10.1029/2011JG001722.
Bowling, D. R., D. E. Pataki, and J. T. Randerson (2008), Carbon isotopes in terrestrial ecosystem pools and CO_2 fluxes, *New Phytol.*, *178*(1), 24–40.

Bowling, D. R., W. J. Massman, S. M. Schaeffer, S. P. Burns, R. K. Monson, and M. W. Williams (2009), Biological and physical influences on the carbon isotope content of CO_2 in a subalpine forest snowpack, Niwot Ridge, Colorado, *Biogeochemistry*, *95*(1), 37–59.
Camarda, M., S. De Gregorio, R. Favara, and S. Gurrieri (2007), Evaluation of carbon isotope fractionation of soil CO_2 under an advective-diffusive regimen: A tool for computing the isotopic composition of unfractionated deep source, *Geochim. Cosmochim. Acta*, *71*(12), 3016–3027.
Carrillo, Y., and E. Pendall (2008), Sources of variation in the carbon isotopic composition of root respiration, paper presented at American Geophysical Union Fall Meeting, AGU, San Francisco, Calif.
Casella, G., and R. L. Berger (2002), *Statistical Inference*, 660 pp., Duxbury, Pacific Grove, Calif.
Cerling, T. E. (1984), The stable isotopic composition of modern soil carbonate and its relationship to climate, *Earth Planet. Sci. Lett.*, *71*(2), 229–240.
Cerling, T. E., D. K. Solomon, J. Quade, and J. R. Bowman (1991), On the isotopic composition of carbon in soil carbon dioxide, *Geochim. Cosmochim. Acta*, *55*(11), 3403–3405.
Clark, J. S. (2003), Uncertainty and variability in demography and population growth: A hierarchical approach, *Ecology*, *84*(6), 1370–1381.
Clark, J. S. (2005), Why environmental scientists are becoming Bayesians, *Ecol. Lett.*, *8*(1), 2–14.
Cox, P. M., R. A. Betts, C. D. Jones, S. A. Spall, and I. J. Totterdell (2000), Acceleration of global warming due to carbon-cycle feedbacks in a coupled climate model, *Nature*, *408*(6813), 750–750.
Dellaportas, P., and D. A. Stephens (1995), Bayesian analysis of errors-in-variables regression models, *Biometrics*, *51*(3), 1085–1095.
Fang, C., and J. B. Moncrieff (1999), A model for soil CO_2 production and transport 1: Model development, *Agric. For. Meteorol.*, *95*(4), 225–236.
Flanagan, L. B., J. R. Brooks, G. T. Varney, S. C. Berry, and J. R. Ehleringer (1996), Carbon isotope discrimination during photosynthesis and the isotope ratio of respired CO_2 in boreal forest ecosystems, *Global Biogeochem. Cycles*, *10*(4), 629–640.
Gamnitzer, U., A. B. Moyes, D. R. Bowling, and H. Schnyder (2011), Measuring and modelling the isotopic composition of soil respiration: Insights from a grassland tracer experiment, *Biogeosciences*, *8*(5), 1333–1350.
Gelman, A., J. B. Carlin, H. S. Stern, and D. B. Rubin (2004), *Bayesian Data Analysis*, 668 pp., Chapman and Hall/CRC Press, Boca Raton, Fla.
Hanson, P. J., N. T. Edwards, C. T. Garten, and J. A. Andrews (2000), Separating root and soil microbial contributions to soil respiration: A review of methods and observations, *Biogeochemistry*, *48*, 115–146.
Heimann, M., and M. Reichstein (2008), Terrestrial ecosystem carbon dynamics and climate feedbacks, *Nature*, *451*(7176), 289–292.
Högberg, P., and D. J. Read (2006), Towards a more plant physiological perspective on soil ecology, *Trends Ecol. Evol.*, *21*(10), 548–554.
Hungate, B. A., E. A. Holland, R. B. Jackson, F. S. Chapin, H. A. Mooney, and C. B. Field (1997), The fate of carbon in grasslands under carbon dioxide enrichment, *Nature*, *388*(6642), 576–579.
Kayler, Z. E., E. W. Sulzman, W. D. Rugh, A. C. Mix, and B. J. Bond (2010a), Characterizing the impact of diffusive and advective soil gas transport on the measurement and interpretation of the isotopic signal of soil respiration, *Soil Biol. Biochem.*, *42*(3), 435–444.
Kayler, Z. E., L. Ganio, M. Hauck, T. G. Pypker, E. W. Sulzman, A. C. Mix, and B. J. Bond (2010b), Bias and uncertainty of $\delta^{13}CO_2$ isotopic mixing models, *Oecologia*, *163*(1), 227–234.
Keeling, C. D. (1958a), The concentration and isotopic abundance of atmospheric carbon dioxide in rural areas, *Geochim. Cosmochim. Acta*, *13*, 322–334.
Keeling, C. D. (1958b), The concentration and isotopic abundances of atmospheric carbon dioxide in rural areas, *Geochim. Cosmochim. Acta*, *13*(4), 322–334.
Kuzyakov, Y. (2006), Sources of CO_2 efflux from soil and review of partitioning methods, *Soil Biol. Biochem.*, *38*(3), 425–448.
Liu, F., M. J. Bayarri, and J. O. Berger (2009), Modularization in Bayesian analysis, with emphasis on analysis of computer models, *Bayesian Anal.*, *4*(1), 119–150.
Lunn, D., D. Spiegelhalter, A. Thomas, and N. Best (2009a), The BUGS project: Evolution, critique and future directions (with discussion), *Stat. Med.*, *28*, 3049–3082.
Lunn, D., N. Best, D. Spiegelhalter, G. Graham, and B. Neuenschwander (2009b), Combining MCMC with 'sequential' PKPD modelling, *Pharmacokinet. Pharmacodyn.*, *36*, 19–38.
Midwood, A. J., and P. Millard (2011), Challenges in measuring the $\delta^{13}C$ of the soil surface CO_2 efflux, *Rapid Commun. Mass Spectrom.*, *25*(1), 232–242.
Moore, J. W., and B. X. Semmens (2008), Incorporating uncertainty and prior information into stable isotope mixing models, *Ecol. Lett.*, *11*(5), 470–480.
Morgan, J. A., D. R. LeCain, A. R. Mosier, and D. G. Milchunas (2001), Elevated CO_2 enhances water relations and productivity and affects gas exchange in C_3 and C_4 grasses of the Colorado shortgrass steppe, *Global Change Biol.*, *7*(4), 451–466.
Mosier, A. R., E. Pendall, and J. A. Morgan (2003), Effect of water addition and nitrogen fertilization on the fluxes of CH_4, CO_2, NO_x, and N_2O following five years of elevated CO_2 in the Colorado Shortgrass Steppe, *Atmos. Chem. Phys.*, *3*, 1703–1708.
Moyes, A. B., S. J. Gaines, R. T. W. Siegwolf, and D. R. Bowling (2010), Diffusive fractionation complicates isotopic partitioning of autotrophic and heterotrophic sources of soil respiration, *Plant Cell Environ.*, *33*(11), 1804–1819.
Nickerson, N., and D. Risk (2009a), A numerical evaluation of chamber methodologies used in measuring the $\delta^{13}C$ of soil respiration, *Rapid Commun. Mass Spectrom.*, *23*(17), 2802–2810.
Nickerson, N., and D. Risk (2009b), Keeling plots are non-linear in non-steady state diffusive environments, *Geophys. Res. Lett.*, *36*, L08401, doi:10.1029/2008GL036945.
Nickerson, N., and D. Risk (2009c), Physical controls on the isotopic composition of soil respired CO_2, *J. Geophys. Res.*, *114*, G01013, doi:10.1029/2008JG000766.
Ogle, K. (2009), Hierarchical Bayesian statistics: Merging experimental and modeling approaches in ecology, *Ecol. Appl.*, *19*(3), 577–581.
Ogle, K., and J. J. Barber (2008), Bayesian data-model integration in plant physiological and ecosystem ecology, *Prog. Bot.*, *69*, 281–311.
Ogle, K., R. L. Wolpert, and J. F. Reynolds (2004), Reconstructing plant root area and water uptake profiles, *Ecology*, *85*(7), 1967–1978.
Ogle, K., J. J. Barber, C. Willson, and B. Thompson (2009), Hierarchical statistical modeling of xylem vulnerability to cavitation, *New Phytol.*, *182*(2), 541–554.
Ogle, K., J. J. Barber, and K. Sartor (2013a), Feedback and modularization in a Bayesian meta-analysis of tree traits affecting forest dynamics, *Bayesian Anal.*, *8*, 133–168.
Ogle, K., C. Tucker, and J. M. Cable (2013b), Beyond simple linear mixing models: Process-based isotope partitioning of ecological processes, *Ecol. Appl.*, doi:10.1890/12-1970.1.
Parnell, A. C., R. Inger, S. Bearhop, and A. L. Jackson (2010), Source partitioning using stable isotopes: Coping with too much variation, *Plos One*, *5*(3), e9672.
Pataki, D. E., J. R. Ehleringer, L. B. Flanagan, D. Yakir, D. R. Bowling, C. J. Still, N. Buchmann, J. O. Kaplan, and J. A. Berry (2003), The application and interpretation of Keeling plots in terrestrial carbon cycle research, *Global Biogeochem. Cycle*, *17*(1), 1022, doi:10.1029/2001GB001850.

Pendall, E., and J. Y. King (2007), Soil organic matter dynamics in grassland soils under elevated CO_2: Insights from long-term incubations and stable isotopes, *Soil Biol. Biochem.*, *39*(10), 2628–2639.

Pendall, E., et al. (2001), Elevated CO_2 stimulates soil respiration in a FACE wheat field, *Basic Appl. Ecol.*, *2*, 193–201.

Pendall, E., et al. (2003), Elevated atmospheric CO_2 effects and soil water feedbacks on soil respiration components in a Colorado grassland, *Global Biogeochem. Cycle*, *17*(2), 1046, doi:10.1029/2001GB001821.

Pendall, E., A. R. Mosier, and J. A. Morgan (2004), Rhizodeposition stimulated by elevated CO_2 in a semiarid grassland, *New Phytol.*, *162*(2), 447–458.

Pendall, E., J. King, A. R. Mosier, J. Morgan, and D. Milchunas (2005), Stable isotope constraints on net ecosystem production in elevated CO_2 experiments, in *Stable Isotopes and Biosphere-Atmosphere Interactions*, edited by L. B. Flanagan, J. R. Ehleringer, and D. E. Pataki, pp. 182–198, Elsevier Sci., San Diego, Calif.

Phillips, D. L., and J. W. Gregg (2001), Uncertainty in source partitioning using stable isotopes, *Oecologia*, *128*, 304.

Quade, J., T. E. Cerling, and J. R. Bowman (1989), Systematic variation in the carbon and oxygen isotopic composition of Holocene soil carbonate along elevation transects in the southern Great Basin, USA, *Geol. Soc. Am. Bull.*, *101*, 464–475.

Risk, D., N. Nickerson, C. L. Phillips, L. Kellman, and M. Moroni (2012), Drought alters respired $\delta^{13}CO_2$ from autotrophic, but not heterotrophic soil respiration, *Soil Biol. Biochem.*, *50*, 26–32.

Shim, J. H., E. Pendall, J. A. Morgan, and D. S. Ojima (2009), Wetting and drying cycles drive variations in the stable carbon isotope ratio of respired carbon dioxide in semi-arid grassland, *Oecologia*, *160*(2), 321–333.

Werth, M., and Y. Kuzyakov (2010), ^{13}C fractionation at the root-microorganisms-soil interface: A review and outlook for partitioning studies, *Soil Biol. Biochem.*, *42*(9), 1372–1384.

Yeakel, J. D., M. Novak, P. R. Guimaraes, N. J. Dominy, P. L. Koch, E. J. Ward, J. W. Moore, and B. X. Semmens (2011), Merging resource availability with isotope mixing models: The role of neutral interaction assumptions, *Plos One*, *6*(7), doi:10.1371/journal.pone.0022015.

Zobitz, J. M., J. P. Keener, H. Schnyder, and D. R. Bowling (2006), Sensitivity analysis and quantification of uncertainty for isotopic mixing relationships in carbon cycle research, *Agric. For. Meteorol.*, *136*(1–2), 56–75.

Zobitz, J. M., S. P. Burns, J. Ogee, M. Reichstein, and R. Bowling (2007), Partitioning net ecosystem exchange of CO_2: A comparison of a Bayesian/isotope approach to environmental regression methods, *J. Geophys. Res.*, *112*, G03013, doi:10.1029/2006JG000282.